Photoinduced phase separation in spin-crossover materials: Numerical simulation of a dynamic photocrystallographic experiment

W. Nicolazzi, S. Pillet,* and C. Lecomte

Laboratoire de Cristallographie, Résonance Magnétique et Modélisations, UMR CNRS 7036, Institut Jean Barriol, Nancy-Université, F-54506 Vandoeuvre-lès-Nancy, France

(Received 18 May 2009; revised manuscript received 29 July 2009; published 12 October 2009)

The dynamics of photoinduced phase transition in spin-crossover materials is studied using numerical simulations of a microscopic two-variable anharmonic model, in close connection with photocrystallographic experiments on the prototype system $[Fe(btr)_2(NCS)_2].H_2O$. A comparative analysis of the simulated diffraction pattern with excitation duration and intensity as variables is performed. Nonlinear dynamics, threshold effect in excitation intensity and light-induced phase separation are modeled and attributed to a strong electron-lattice coupling, mediated by long-range elastic interactions. Photoinduced nucleation and domain growth of the metastable high-spin phase is evidenced and quantitatively explained in the Avrami formalism.

DOI: 10.1103/PhysRevB.80.132102 PACS number(s): 64.60.De, 05.50.+q, 75.30.Wx, 75.60.−d

A considerable interest is currently attached to photoinduced phenomena in strongly correlated electron molecular materials.[1–4] Various phase-transition processes triggered by light have been reported, for which photoexcitation results in a macroscopic phase change. These so-called photoinduced phase transitions (PIPTs) originate from strong electron (or spin)-lattice coupling, and may present nonlinear photoexcitation and relaxation dynamics, characterized by the existence of a threshold behavior in absorbed photon intensity, an incubation period and possibly phase separation.[5,6]

Spin-crossover (SC) molecular Fe(II) complexes are one of the most relevant materials exhibiting a reversible photoinduced conversion between a fundamental low-spin (LS: $S=0$) state and a metastable high-spin (HS: $S=2$) state.[7] Most of their solid-state properties are closely related to cooperative interactions of elastic origin within the crystal lattice. Nonlinear LS to HS photoexcitation dynamics,[5,6] and characteristic sigmoidal relaxations[8,9] have been reported for highly cooperative systems, this can be well formulated in a macroscopic evolution equation.[10] Intensive theoretical work addressed the question of the cooperativity. In the elasticity theory, the interaction consists of a long-range contribution, originating from the image pressure,[11] and short-range correlations between neighboring molecules.[12] Several microscopic Ising-like models were developed;[13–16] they can explain most of the SC properties in the static regime. More recently, cooperative elastic models have been introduced using various approaches,[17–24] one-dimensional atom-phonon coupling,[17] molecular dynamics,[18,19] or lattice distortion model.[22,23] Several theoretical studies, tackled the dynamics of spin transition in the photoinduced and relaxation regimes.[15,16,22–24] These models can capture the nonlinear dynamics, threshold effect in excitation intensity and incubation period. It has been argued that like spin domains (LSDs) may play a key role in the cooperative spin-transition process, resulting in phase-separation phenomena. Although thermally and photoinduced phase separation has indeed been reported for several SC materials,[25–30] the condition for the development of LSDs as well as their nucleation and growth dynamics is still an open question.

We investigate the nonlinear dynamics of the PIPT process in SC materials using $[Fe(btr)_2(NCS)_2].H_2O$ as a representative example for highly cooperative two-dimensional (2D) systems. $[Fe(btr)_2(NCS)_2].H_2O$ exhibits LS to HS PIPT at very low temperature, characterized by a drastic expansion of the unit-cell volume, and 3.7% increase in Fe…Fe separation distance.[29] Thermocrystallographic and photocrystallographic experiments have clearly evidenced the presence of LSDs, whose growth kinetics follows the Avrami model.[25,28] We focus hereafter on the photoinduced dynamics of LSD nucleation and growth in the low-temperature regime using numerical simulation, in close connection with these experimental results.

The simulations presented here are based on the elastic Ising-like model introduced previously,[21] we recall here only the main aspects. We consider the Ising-like formalism of fictitious spin operators σ on a square lattice[13–15] which we take as deformable. The vibronic HS and LS states of Fe(II) are represented by $\sigma=+1$ and -1, respectively. The on-site Hamiltonian which accounts for the inner degrees of freedom of N SC entities writes

$$\mathcal{H}_0 = \frac{\Delta_{eff}(T)}{2}\sum_{i=1}^{N}\sigma_i, \tag{1}$$

where $\Delta_{eff}(T)=\Delta-k_BT\ln(g)$, with Δ the HS-LS difference in ligand-field energy and $g=g_+/g_-\gg 1$ the effective degeneracy ratio, related to the LS to HS electronic and vibrational entropy increase $\Delta S=k_B\ln(g)$. The elastic interaction, responsible for the cooperativity, is introduced as follows. The position $\vec{r}_i$ of each SC entity is variable, allowing for lattice distortion and molecular volume change associated to the spin-state switching. The interaction energy is assumed to depend on the spin state σ_i and relative position $\vec{r}_i$ of the SC molecules, it can be written as

$$\mathcal{H}_{int}(\{\sigma\},\{\vec{r}\}) = \sum_{\langle i,j\rangle} A(\sigma_i,\sigma_j)V_{elast}(r_{\langle i,j\rangle},r^0_{\langle i,j\rangle}), \tag{2}$$

where the sum runs over all nearest-neighbor pairs $\langle i,j\rangle$. $r_{\langle i,j\rangle}=\|\vec{r}_j-\vec{r}_i\|$ and $r^0_{\langle i,j\rangle}=\|\vec{r}^0_j-\vec{r}^0_i\|$ are the intersite instantaneous and equilibrium distance, respectively. The equilibrium distance $r^0_{\langle i,j\rangle}$ in the undistorted lattice and the elastic coupling

$A(\sigma_i, \sigma_j)$ between a pair of sites i and j depend on their spin state to account for the difference in Fe…Fe distances and elastic constants between purely HS and purely LS phases. $A(\sigma_i, \sigma_j)$ can be formally rearranged to

$$A(\sigma_i, \sigma_j) = J_0 + J_1(\sigma_i + \sigma_j) + J_2\sigma_i\sigma_j. \quad (3)$$

V_{elast} in Eq. (2) takes the form of an anharmonic intersite potential of the empirical (6)–(3) Lennard-Jones type with finite range.

For the present out-of-equilibrium treatment, we consider two transition processes, a thermal one and an optical one. The thermal switching of spin and lattice variable is described by a nonconserved order parameter dynamics of the Arrhenius type.[14] A one-step dynamic is adopted, which corresponds to the transition probability from an initial configuration of energy E_i to a final configuration of energy E_f through a saddle point of energy E_T.

$$W_{spin}^{therm}(\{\sigma\} \to \{\sigma'\}) = \frac{1}{\tau_{spin}^0} e^{-\beta[E_{intra}^0 - E_i]}, \quad (4)$$

with E_{intra}^0 a constant intramolecular vibronic energy barrier. A similar formalism is introduced for the lattice variable as

$$W_{elast}^{therm}(\{\vec{r}\} \to \{\vec{r'}\}) = \frac{1}{\tau_{elast}^0} e^{-\beta[E_{elast} - E_i/2]}. \quad (5)$$

Contrary to E_{intra}^0, $E_{elast}=(E_{elast}^0+\frac{E_f}{2})$ is locally defined and depends on the final spin and lattice configuration.

The optical excitation, which is considered as a single site and unidirectional (LS to HS) process, is introduced in the spin-switching dynamics.[15] A phenomenological transition rate W_{spin}^{opt} is simply added to Eq. (4), considering thermal and optical phenomena as decoupled.

$$W_{spin}^{opt} = \frac{I_0 S}{2}(1 - \sigma_i). \quad (6)$$

I_0 is the incident excitation intensity and S the absorption cross-section accounting also for the photoexcitation quantum efficiency. Following previous investigations on the equilibrium behavior of our Hamiltonian,[21] we chose values of the interaction constants $J_0=998.85$, $J_1=0.15$, and $J_2=2.15$ such as to reproduce abrupt thermal spin transitions with large hysteresis in agreement with the magnetic behavior of $[Fe(btr)_2(NCS)_2].H_2O$. At $t=0$, the system, prepared in the LS state, is set in contact with the thermal bath at $T=1.5$, below the order-disorder transition of the model,[21] and the excitation intensity turned on ($I_0 \neq 0$). The behavior of the system is analyzed using the usual HS fraction n_{HS} and a normalized lattice spacing r^{norm}; both take value 0 and 1 in purely LS and HS phases, respectively.

X-ray diffraction measurements, conducted as a function of time under CW laser excitation ($T=15$ K, $\lambda=488$ nm), have shown a systematic splitting of all Bragg peaks [inset Fig. 4(a)], which is attributed to a heterogeneous phase-transition mechanism with light-induced HS and LS phase separation.[25,28] For strong J_2 coupling, our simulations present such a light-induced structural phase separation (Fig. 1). The PIPT proceeds successively by a nucleation of HS structural domains within the LS matrix, followed by a domain growth stage. Structural relaxation occurs at the domain walls, to accommodate the large HS to LS lattice spacing misfit. At $t=0$, the distribution of lattice spacing exhibits a single sharp peak centered at the LS value ($r^{norm} \approx 0$) (Fig. 1 bottom). As the PIPT proceeds, the distribution broadens and a second broad peak centered at the HS value ($r^{norm} \approx 1$) develops. The double peak features evidence a structural phase-separation process, while the broadening characterizes the buildup of inhomogeneous lattice strain due to short-range correlations. Lattice strain is relaxed at completeness of the PIPT.

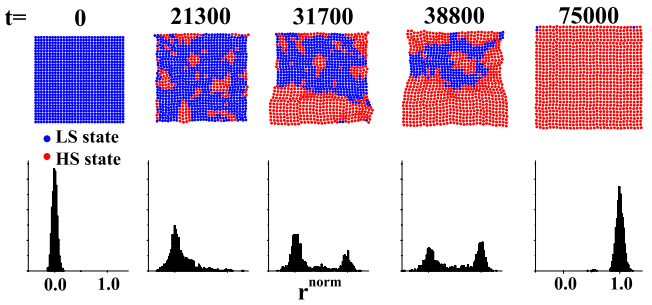

FIG. 1. (Color online) (Top) snapshots of the system as a function of time (in MCS) under continuous light excitation $I_0=0.0109$. (Bottom) distribution of intersite distances $r_{\langle i,j\rangle}^{norm}$ showing the double maxima distribution related to light-induced phase separation.

On the course of the PIPT, the evolution of the spin and lattice variables both exhibits a nonlinear sigmoidal trend [Fig. 2(a)]. In the first stage, the rate of photoexcitation is quite reduced; this is the incubation time during which nucleation occurs. Then the phototransformation speeds up, criti-

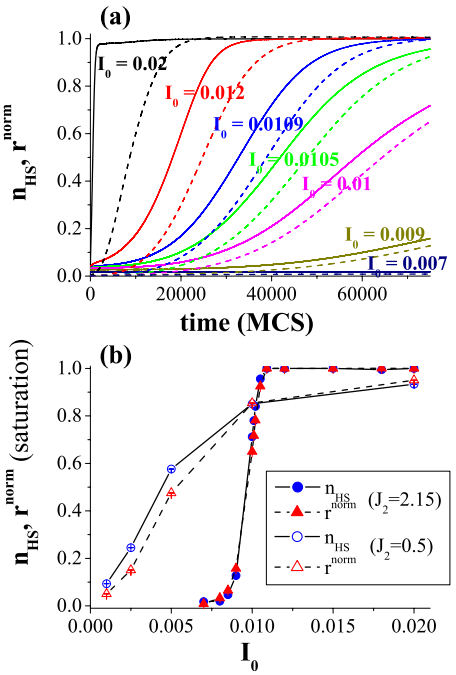

FIG. 2. (Color online) (a) Kinetics of photoexcitation as a function of optical excitation intensity I_0 (n_{HS} as continuous line, r^{norm} as dashed line), (b) conversion efficiency: n_{HS} and r^{norm} values at the pseudosaturation ($t=75\,000$ MCS).

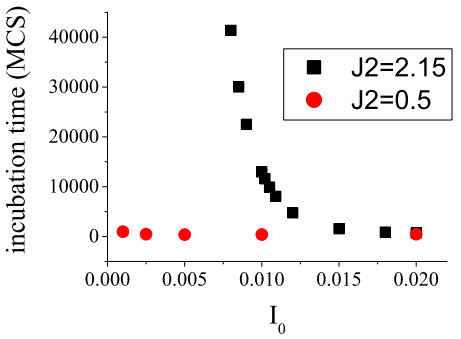

FIG. 3. (Color online) Incubation time as a function of optical excitation intensity I_0, for weak (J_2=0.5) and strong (J_2=2.15) cooperativities.

cal nuclei are formed through optically induced fluctuations, and grow to metastable HS domains. In the present case, cooperativity plays a paramount role in the photoexcitation process. For such cooperative SC materials, the possibility for a nonconstant photoexcitation quantum yield [S becoming dependent on n_{HS} in Eq. (6)] has been argued.[31]

It has been observed experimentally,[29] that there exist a high threshold photon density below which no phase change is triggered for $[Fe(btr)_2(NCS)_2].H_2O$ at 15 K. In our simulations, we observe that indeed for low values of I_0 ($I_0<0.007$), no photoconversion occurs; as I_0 increases, the transformation rate increases considerably, and the incubation time shortens [Fig. 2(a)]. A threshold effect in excitation intensity is clearly evidenced. We plot in Fig. 2(b) the photoconversion efficiency, that is the values of r^{norm} and n_{HS} at the pseudosaturation [taken as t=75 000 Monte Carlo steps (MCS)], and compare them to a weakly cooperative case (J_2=0.5). The photoconversion efficiency is nonlinear in excitation intensity, the threshold behavior appears quite abrupt, with a drastic increase in efficiency in a narrow range of I_0 around 0.009. This is comparable to the observation from photocrystallographic experiments. On the contrary, no threshold behavior is observed for the weakly cooperative case, which proves that strong elastic interactions are at the origin of the nonlinear kinetics and threshold effect. The threshold effect may be explained as follows. Owing to the large LS to HS unit-cell misfit ($r^0_{HS}>r^0_{LS}$), large strain energy is associated to each HS nucleus forming within the LS structural matrix. High photon density is required to provide a critical HS nucleus with sufficient lifetime, stabilized by the strong cooperativity, which may further grow to a macroscopic HS phase.

The incubation time, taken arbitrarily as the time required for a n_{HS}=0.01 conversion, is highly dependent on the excitation intensity I_0 and intersite cooperative interactions J_2 as given in Fig. 3. For weak cooperativity, the incubation time is nearly negligible whatever the excitation intensity, a homogeneous nucleation occurs, while domain growth is hindered. For strong cooperativity and weak excitation, the incubation time is almost infinite, no PIPT is observed, the formed nuclei never reach the critical size to become stable. As the excitation intensity increases above I_0=0.009, n_{HS} inhomogeneities develop and the lifetime of the critical nuclei considerably decreases, the incubation time shortens.

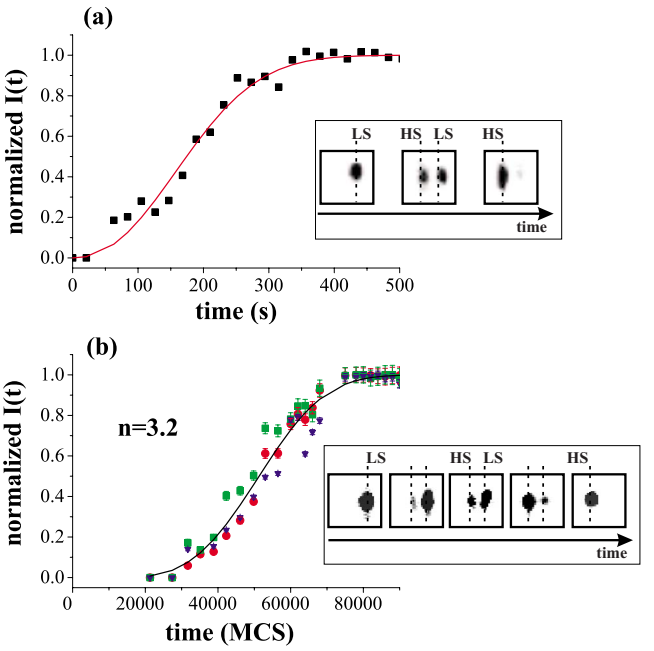

FIG. 4. (Color online) Avrami fit to the normalized HS Bragg peak intensity (dots): $[I(t)-I(t\to\infty)]/[I(t\to\infty)-I(t\to 0)]$. (a) Photocrystallographic experimental results, Ref. 25, (b) numerical simulation (I_0=0.0109). n is the Avrami exponent. Insets: splitting of a Bragg peak under continuous light excitation.

To interpret the dynamic photocrystallographic results,[25] we have calculated the 2D diffraction pattern for each configuration of our simulations using an appropriate Fourier transform procedure.[32,33] First, the splitting of the Bragg peaks observed experimentally on the course of the PIPT is well reproduced (Fig. 4 insets), the HS domains developing within the LS matrix (Fig. 1 top) are large enough and structurally coherent to result in a diffracted signal. In the case of small or structurally disordered HS domains, diffuse features would rather be observed. The progress of the PIPT was monitored by the evolution of the HS Bragg peak intensity, which is in a first approximation proportional to the overall volume of the HS phase. The experimental and simulated kinetics (Fig. 4) follow the Kolmogorov–Johnson–Mehl–Avrami model[25,34] quite well:

$$I_{HS}(t) \propto V_{HS}(t) = 1 - \exp\{-[k(t-\tau)]^n\}, \qquad (7)$$

with τ the incubation time, k the transformation rate constant, and n the Avrami exponent. The fitted Avrami exponent of 3.2 is characteristic of a perfect 2D nucleation and growth mechanism ($n=d+1$), where d is the dimension of the process, in line with the 2D structural topology. Altogether, the Bragg peak splitting and Avrami kinetics correlate perfectly with a PIPT driven by nucleation and growth of LSDs.

In summary, we have investigated the light-induced phase-separation phenomenon in SC molecular solids using numerical simulations of a two-variable anharmonic model. Elastic models, similar to ours, with nonetheless spin-independant interactions can reproduce the threshold effect and incubation period, but the photoinduced phase-separation process is usually not observed,[22,24] especially

when only long-range interactions are accounted for. Some of these models even presents a mean-field critical behavior.[35] The only conditions under which phase separation has been characterized is in a model introducing volume-striction effects with a fixed system volume.[23] Such volume striction is inherent to our model with open boundary conditions. Our scheme with elastic couplings dependent on the spin and separation distance introduces explicitly inhomogeneities and a spatial distribution and fluctuation of interaction constants, which probably drives the macroscopic structural phase separation for strong interactions. The model captures the essential features of dynamic photocrystallographic experiments such as Bragg peak splitting and nonlinear photoconversions. The threshold behavior in excitation intensity and incubation time are driven by LSDs nucleation and growth whose kinetics follows the Avrami model. This is undoubtedly of current interest for getting insights on the switching dynamics from bulk SC materials down to SC nanoparticles, for which the role of LSDs may severely differ.

This work was supported by the European Network of Excellence MAGMANet (Grant No. FP6-515767-2), the Université Henri Poincaré, the CNRS, and the Institut Jean Barriol. W.N. is grateful to the Ministère de la Recherche.

*Corresponding author; sebastien.pillet@lcm3b.uhp-nancy.fr

[1] E. Collet, M. H. Lemee-Cailleau, M. Buron-Le Cointe, H. Cailleau, M. Wulff, T. Luty, S. Koshihara, M. Meyer, L. Toupet, P. Rabiller, and S. Techert, Science **300**, 612 (2003).
[2] H. Matsuzaki, W. Fujita, K. Awaga, and H. Okamoto, Phys. Rev. Lett. **91**, 017403 (2003).
[3] S. Iwai, S. Tanaka, K. Fujinuma, H. Kishida, H. Okamoto, and Y. Tokura, Phys. Rev. Lett. **88**, 057402 (2002).
[4] H. Liu, A. Fujishima, and O. Sato, Appl. Phys. Lett. **86**, 122511 (2005).
[5] Y. Ogawa, S. Koshihara, K. Koshino, T. Ogawa, C. Urano, and H. Takagi, Phys. Rev. Lett. **84**, 3181 (2000).
[6] Y. Moritomo, M. Kamiya, A. Nakamura, A. Nakamoto, and N. Kojima, Phys. Rev. B **73**, 012103 (2006).
[7] A. Hauser, J. Chem. Phys. **94**, 2741 (1991).
[8] A. Hauser, Chem. Phys. Lett. **192**, 65 (1992).
[9] A. Hauser, J. Jeftic, H. Romstedt, R. Hinek, and H. Spiering, Coord. Chem. Rev. **190-192**, 471 (1999).
[10] F. Varret, K. Boukheddaden, E. Codjovi, C. Enachescu, and J. Linares, *Topics in Current Chemistry* (Springer-Verlag, Berlin, 2004), Vol. 234, p. 199.
[11] H. Spiering, *Topics in Current Chemistry* (Springer-Verlag, Berlin, 2004), Vol. 235, p. 171.
[12] H. Spiering, T. Kohlhaas, H. Romstedt, A. Hauser, C. Bruns-Yilmaz, J. Kusz, and P. Gutlich, Coord. Chem. Rev. **190-192**, 629 (1999).
[13] A. Bousseksou, H. Constant-Machado, and F. Varret, J. Phys. I **5**, 747 (1995).
[14] K. Boukheddaden, I. Shteto, B. Hôo, and F. Varret, Phys. Rev. B **62**, 14796 (2000).
[15] K. Boukheddaden, I. Shteto, B. Hôo, and F. Varret, Phys. Rev. B **62**, 14806 (2000).
[16] H. Romstedt, A. Hauser, and H. Spiering, J. Phys. Chem. Solids **59**, 265 (1998).
[17] J. A. Nasser, Eur. Phys. J. B **21**, 3 (2001).
[18] M. Nishino, K. Boukheddaden, Y. Konishi, and S. Miyashita, Phys. Rev. Lett. **98**, 247203 (2007).
[19] M. Nishino, K. Boukheddaden, and S. Miyashita, Phys. Rev. B **79**, 012409 (2009).
[20] Y. Konishi, H. Tokoro, M. Nishino, and S. Miyashita, Phys. Rev. Lett. **100**, 067206 (2008).
[21] W. Nicolazzi, S. Pillet, and C. Lecomte, Phys. Rev. B **78**, 174401 (2008).
[22] O. Sakai, T. Ogawa, and K. Koshino, J. Phys. Soc. Jpn. **71**, 978 (2002).
[23] O. Sakai, M. Ishii, T. Ogawa, and K. Koshino, J. Phys. Soc. Jpn. **71**, 2052 (2002).
[24] T. Kawamoto and S. Abe, Phys. Rev. B **68**, 235112 (2003).
[25] S. Pillet, V. Legrand, M. Souhassou, and C. Lecomte, Phys. Rev. B **74**, 140101(R) (2006).
[26] F. Varret, K. Boukheddaden, C. Chong, A. Goujon, B. Gillon, J. Jeftic, and A. Hauser, EPL **77**, 30007 (2007).
[27] K. Ichiyanagi, J. Hebert, L. Toupet, H. Cailleau, P. Guionneau, J.-F. Létard, and E. Collet, Phys. Rev. B **73**, 060408(R) (2006).
[28] S. Pillet, J. Hubsch, and C. Lecomte, Eur. Phys. J. B **38**, 541 (2004).
[29] V. Legrand, S. Pillet, C. Carbonera, M. Souhassou, J.-F. Létard, P. Guionneau, and C. Lecomte, Eur. J. Inorg. Chem. **36**, 5693 (2007).
[30] N. Huby, L. Guérin, E. Collet, L. Toupet, J. C. Ameline, H. Cailleau, T. Roisnel, T. Tayagaki, and K. Tanaka, Phys. Rev. B **69**, 020101(R) (2004).
[31] C. Enachescu, U. Oetliker, and A. Hauser, J. Phys. Chem. B **106**, 9540 (2002).
[32] B. D. Butler and T. R. Welberry, J. Appl. Crystallogr. **25**, 391 (1992).
[33] T. Proffen and R. B. Neder, J. Appl. Crystallogr. **30**, 171 (1997).
[34] M. Avrami, J. Chem. Phys. **7**, 1103 (1939); **8**, 212 (1940).
[35] S. Miyashita, Y. Konishi, M. Nishino, H. Tokoro, and P. A. Rikvold, Phys. Rev. B **77**, 014105 (2008).